

Evaluation of anticancer activity of *Annona muricata* leaf targeting FGFR3 and EGFR receptors against bladder and lung cancer

Pattilthodika Suhail^{1,2*} , Velappan Venkatachalam Venkatachalam² , Thirumalaisamy Balasubramanian¹ , Radhakrishnan Murali² , Arvind Babu Lalpet Renganathan³ 

¹Department of Pharmacology, Al Shifa College of Pharmacy, Perinthalmanna, India.

²Department of Pharmacy, Annamalai University, Chidambaram, India.

³Department of Computer and Information Science, Annamalai University, Chidambaram, India.

ARTICLE HISTORY

Received on: 15/11/2024
Accepted on: 11/02/2025
Available Online: 05/03/2025

Key words:

Annona muricata, bladder cancer, EGFR proteins, FGFR3 proteins, lung cancer, MTT assay, molecular docking.

ABSTRACT

The amplification of tyrosine kinase receptors, specifically fibroblast growth factor receptors and epidermal growth factor receptors, is primarily observed in various cancers, including bladder and lung cancer. This study aimed to identify the phytochemical components of *Annona muricata* leaves and evaluate their anticancer potential. The study used Q-TOF LC/MS analysis to identify phytochemical components and conducted molecular docking studies to predict the binding action of quinic acid. The largest peak was found at a retention time of 10.12 (stephabyssine), followed by 9.97 (procyanidin B2) and 11.83 (quinic acid) minutes, revealing the presence of many phytochemicals. In molecular docking studies, quinic acid was found to interact with the catalytic residues of LEU 478, ALA 557, LYS 476, and ALA 559 with hydrogen bonds, indicating hydrophobic interaction with some amino acids in the hydrophobic pockets of fibroblast-growth factor receptors 3 protein with a docking score of -9.94 Kcal/mol. It also interacts with the catalytic residues of ASP 831, THR 830, and THR 766 of the epidermal growth factor receptors proteins with a docking score of -9.103 Kcal/mol. The assessment of anticancer activity was conducted through the measurement of mitochondrial dehydrogenase activity (3-(4, 5-dimethylthiazol-2-yl)-2, 5-diphenyltetrazolium bromide assay). The IC_{50} for MCF-7, T47D, HCT-15, and PC-3 were found to be 76.64 ± 2.56 , 142.43 ± 1.86 , 42.68 ± 2.89 , and 152.16 ± 3.21 μ g/ml, respectively. The findings were corroborated by the observed morphological alterations, including membrane blebbing, cell detachment, and rounded cell morphology in comparison to parental cells. The phytochemical analysis, including *in vitro* and *in silico* studies, identified significant constituents and key mechanisms of quinic acid as a potential anticancer agent derived from *A. muricata* leaves.

INTRODUCTION

Bladder cancer is mainly treated by surgery, but the high risk of treatment failure in both the advanced and early stages of the illness has sparked interest in using a mix of different treatment methods in different clinical situations to enhance results. Neoadjuvant multi-agent chemotherapy has shown significant advantages for locally advanced illness,

namely in terms of disease response and survival [1]. The primary cause of lung cancer fatalities connected to cancer, accounting for 27% of all deaths of cancer. Adenocarcinoma is the predominant kind of lung cancer. Numerous driving alterations that facilitate the initiation and progression of malignant tumors have been identified [2].

The tyrosine kinase receptors, epidermal growth factor receptors (EGFRs), and fibroblast-growth factor receptors (FGFRs) possess both intracellular and extracellular tyrosine kinase domains. FGF receptors mainly include FGFR1, FGFR2, FGFR3 and FGFR4 [3]. Among the 90 identified genes that encode proteins with tyrosine kinase activity, receptors including vascular endothelial growth factor, platelet derived growth factor, and hepatocyte growth factor are notably associated with malignant diseases [3]. Numerous physiological processes, such

*Corresponding Author

Pattilthodika Suhail, Department of Pharmacology, Al Shifa College of Pharmacy, Perinthalmanna, India and Department of Pharmacy, Annamalai University, Chidambaram, India.
E-mail: ptsuhl@gmail.com

as the development of embryos, fetal organogenesis, development during early life, metabolic balance, and regeneration and repair of tissue, are influenced by FGFR signaling. Cancer cells may acquire the abnormal activation of this signaling pathway by processes such as FGFR family member exon amplification, fusion, or missense mutations [4].

As transmembrane proteins with intrinsic, non-permanent enzymatic activity, FGFRs serve a purpose in normal, cancer-free cells. Adenocarcinoma [5], bladder cancer [6], colorectal cancer [7], prostate cancer [8], and breast cancer [8,9] are among the most common malignancies that have FGFR1 amplifications. To maximize their effectiveness, small molecule inhibitors and alternative therapeutic approaches including ligand traps, antibody-based therapies, and RNA/DNA aptamers should target FGFRs first and foremost [10–12].

By activating crucial oncogenic pathways like the Ras-Raf-Mek and PI3K/Akt-mTOR pathways, the downstream signaling of EGFR has been identified as a crucial factor in the development of cancerous phenotype. The continual activation of the receptor is very necessary for cancer cells with EGFR-activating mutations to keep them malignant [9]. Consequently, substantial efforts have been dedicated to the development of EGFR inhibitors, often using chemicals that interact with either the ATP or the enzyme-substrate binding region to suppress tyrosine kinase phosphorylation.

Annona muricata Linn. (*A. muricata*) includes a variety of bioactive elements that might be candidates to inhibit several anti-apoptotic proteins. It has been suggested that this tropical plant can encourage apoptosis in several cancer cell types [13–16]. Acetogenins and other bioactive chemical classes, as well as alkaloids, control this activity. For instance, in hepatocellular carcinoma (HepG2) cells, acetogenins have been demonstrated to cause apoptotic cell death by inhibiting mitochondrial complex I [17,18]. This research was done to evaluate the anticancer activity of *A. muricata* leaves using *in silico* and *in vitro* experimental models, considering the demand for innovative antitumor agents.

METHODOLOGY

Plant collection

Annona muricata leaves samples were gathered from different parts of western ghats like Malappuram (11.0510°-N, 76.0711°-E), Wayanad (11.6994°-N, 76.0773°-E), Nelliampathy areas (10.5354°-N, 76.6936°-E) and verified by the Scientist from Division of Pharmacognosy, Arya Vaidyasala, Kottakkal, Malappuram, Kerala, India. A dried plant specimen was kept in the Herbarium of Centre for Medicinal Plant Research, Arya Vaidyasala, Kottakkal (No. 10045).

Plant extract preparation

After being cleaned with distilled water, the leaves were oven dried at 60°C before being crushed into a coarse powder with a diameter of about 1 mm. A conical flask containing 100 g of ground material, and 500 ml of 96% ethanol was shaken intermittently for 72 hours. The resultant extract was evaporated at 50 rpm and 40°C using a rotary evaporator, the obtained concentrated extract was then protected from

deterioration by being kept in a refrigerator at 4°C until it was needed again.

Q-TOF LC/MS analysis

The phytochemicals present in the ethanolic extract of the *A. muricata* leaves (EAML) were initially identified [19], and their identities were then validated by Q-TOF LC-MS. The analysis was then carried out using Mariner Bio spectrometry, which is fitted with a binary pump. An ESI source-equipped Q-TOF mass spectrometer (Agilent 1260 Infinity I) was connected to the HPLC. A 140°C source temperature was selected for full-scan operation from *m/z* 100 to 1,200. For the analysis, a Phenomenex 5 μ C8 HPLC column (150 \times 2 mm) was employed. Ethanol was the solvent, while formic acid was 0.3%. The overall flow rate of solvent delivery was 0.1 ml/minute. Isocratic elution was employed to operate the solvent. The positive ion technique was used to acquire the MS spectra [20,21].

Protein and ligand structure retrieval and molecular docking

The X-ray crystal structures of FGFR (PDB ID: 4K33) and EGFR (PDB ID: 1M17) were downloaded from the PDB (<https://www.rcsb.org/>), while the chemical structure of quinic acid was retrieved from Pub-Chem database (<https://pubchem.ncbi.nlm.nih.gov>). Protein development Wizard in Epik version 3.4 processed the protein structure, facilitating the development of the crystal structure for ionization, hydrogen bond optimization, heterogeneous state formation, protonation, completion of missing loops and side chains (utilizing Prime), and overall minimization. The receptor grid generation panel of Glide version 6.9 produced the grid around active sites. The default grid size was 20 Å, with grid points preserved along the *x*, *y*, and *z* axes. All docking and scoring calculations were conducted using Glide version 6.9 inside Schrodinger Maestro version 10.4. In this work, the active site of the protein was configured to adapt to 5 Å for the ligand suitably. The simulation period was 25 nanoseconds.

In vitro anticancer activity

The breast cancer cell lines (MCF 7, T47D), colorectal cancer cell lines (HCT-15), and prostate cancer cell lines (PC3), are supplied by National Centre for Cell Science. Cell lines were maintained in dulbecco's modified eagle medium supplemented with 10% foetal bovine serum, along with 100 g/ml of streptomycin and penicillin (100 U/ml). The environmental parameters for all cell cultures were maintained at 37°C, with 5% CO₂, air of 95%, and 100% relative humidity. Anticancer activity of EAML was assessed using an 3-(4, 5-dimethylthiazol-2-yl)-2, 5-diphenyltetrazolium bromide (MTT) assay with these cell lines, and untreated cells were used as control [22]. A 12-well plate containing medium was inoculated with approximately 1 \times 10⁵ cells incubated for 24 hours at 37°C. The cells were subjected to different extract concentrations while maintaining consistent temperature and duration. Each well was treated with 100 μ l of MTT and subsequently incubated for a duration of 4 hours. One ml solubilization solution comprising isopropanol, HCl, and Triton

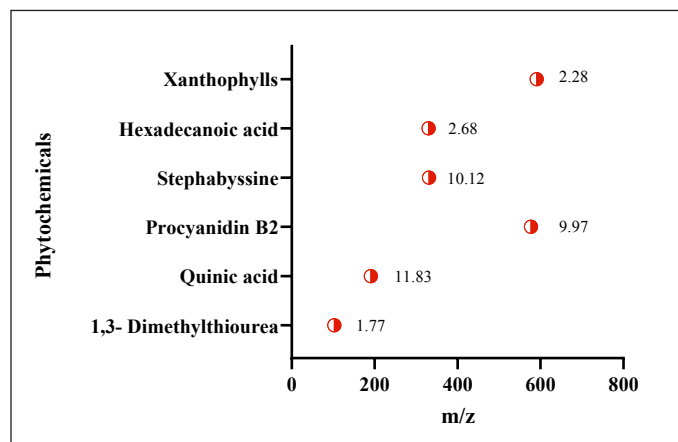


Figure 1. Presents of phytochemicals in *A. muricata* leaf from Q-TOF LC/MS analysis with retention time.

X 100 was employed to dissolve the dark blue formazan crystals through ceaseless aspiration and re-suspension. The absorbance of the colored product was measured at 570 nm. The study of cytotoxicity included an analysis of the ratio of the treated cell population that perished in comparison to the untouched control, as demonstrated by their relative absorbance analyzed via the MTT assay. Three experiments were conducted with duplicate runs, yielding equivalent outcomes and the values are expressed as mean \pm standard error ($n = 3$).

To investigate the alterations in morphological characteristics, MCF-7 cells have been prepared and incubated for 24 hours. Following extract, the specimens underwent washing and were subsequently stained using a solution that included both acridine orange (AO) and ethidium bromide (EB). The level of fluorescence detected in the cells was assessed using a fluorescence microscope and ocular lens. The cells were subsequently pelleted, subjected to three washes, and then stained with AO and EB. The subsequent phase involved observing the cells using a fluorescent microscope equipped with 20X objectives.

Absorption, distribution, metabolism, excretion, and toxicity (ADMET) prediction

To evaluate the ligands' physiological activity, it is essential to analyze their ADMET characteristics. The QikProb tool, version 3.0, developed by Schrodinger, was used to assess the ADMET properties of the ligands.

RESULTS AND DISCUSSION

Q-TOF LC/MS analysis

Initial phytoconstituent investigations indicated the presence of flavonoids and glycosides in the EAML. **Figure 1** displays the significant chemicals discovered using Q-TOF LC-MS analysis. The largest peak was found at a retention time of 10.12 (stephabysine), followed by 9.97 (procyanidin B2) and 11.83 (quinic acid) minutes. The m/z readings reveal the presence of many phytochemicals, including quinic acid (191 m/z), among others.

Table 1. Docking score and RMSD value of quinic acid on FGFR3 (PDB ID: 1E8W), and EGFR (PDB ID: 1M17) proteins.

Compound	Docking score (Kcal/mol)		RMSD(A ^o)
	4K33	1M17	
Quinic acid	-9.94	-9.103	0.196

Quinic acid, a significant natural cyclitol, is present in a variety of well-known healthful foods, including fruits, vegetables, tea, and coffee [23]. According to biological research, quinic acid can chelate transition metals and has anti-inflammatory, antioxidant, and antimutagenic properties [24].

Molecular modeling study

Molecular modeling and dynamics of quinic acid were conducted on FGFR3 and EGFR, which are implicated in several malignancies, including bladder and lung cancer [25]. These enzymes initiate several signaling cascades implicated in the aetiology of bladder and lung cancer [25]. The docking procedure was confirmed by redocking the native ligand to FGFR3 (PDB ID: 4K33) and EGFR (PDB ID: 1M17). The root mean square deviation (RMSD) of the ligand was found to be under 2 Å, suggesting that the employed technique was effectively validated [26,27]. The binding energy of quinic acid is shown in **Table 1**.

Docking study on FGFR3 proteins

In early-phase trials, 10% of patients with FGFR mutations demonstrated significant benefits from FGFR-targeted therapies; however, the overall response rates remained largely inadequate, despite promising preclinical study outcomes. In clinical trials, FGFR amplification that do not result in alterations in protein expression, the activation of alternative signaling pathways, the development of secondary drug-resistant FGFR mutations, and/or intratumoral heterogeneity, including FGFR-independent subclones, have impeded the effectiveness of FGFR-targeted therapies [28]. In this study, quinic acid was found to interact with the catalytic residues of LEU 478, ALA 557, LYS 476, and ALA 559 with hydrogen bonds, indicating hydrophobic interaction with some amino acids in the hydrophobic pockets of FGFR3, as shown in **Figure 2**. The calculated binding energy of quinic acid was -9.94 Kcal/mol, indicating its interaction with FGFR3 proteins and anti-bladder cancer activity [28].

Docking study on EGFR proteins

The Ras-Raf-Mek and PI3K-Akt-mTOR pathways, associated with proliferation, survival, invasiveness, metastatic spread, and tumor angiogenesis, are two essential oncogenic pathways activated by EGFR downstream signaling, significantly contributing to the malignant phenotype [29]. Cancer cells harboring EGFR-activating mutations exhibit complete reliance on sustained receptor activation for the preservation of their malignancy [30]. The hydrogen bonding interactions between the ligand and EGFR protein are illustrated in **Figure 3**. The quinic acid was found to interact with the catalytic residues of ASP 831, THR 830, and THR 766

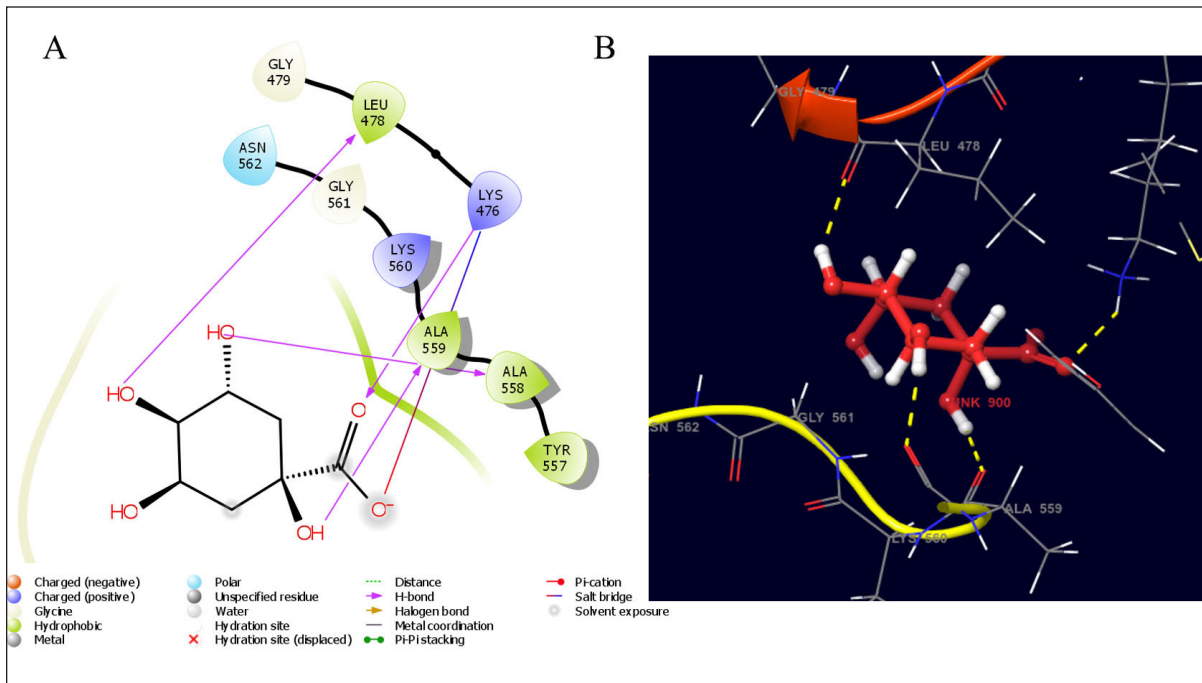


Figure 2. The estimated binding geometry of quinic acid on the active site of FGFR3, (A and B) 2D and 3D structures of interaction.

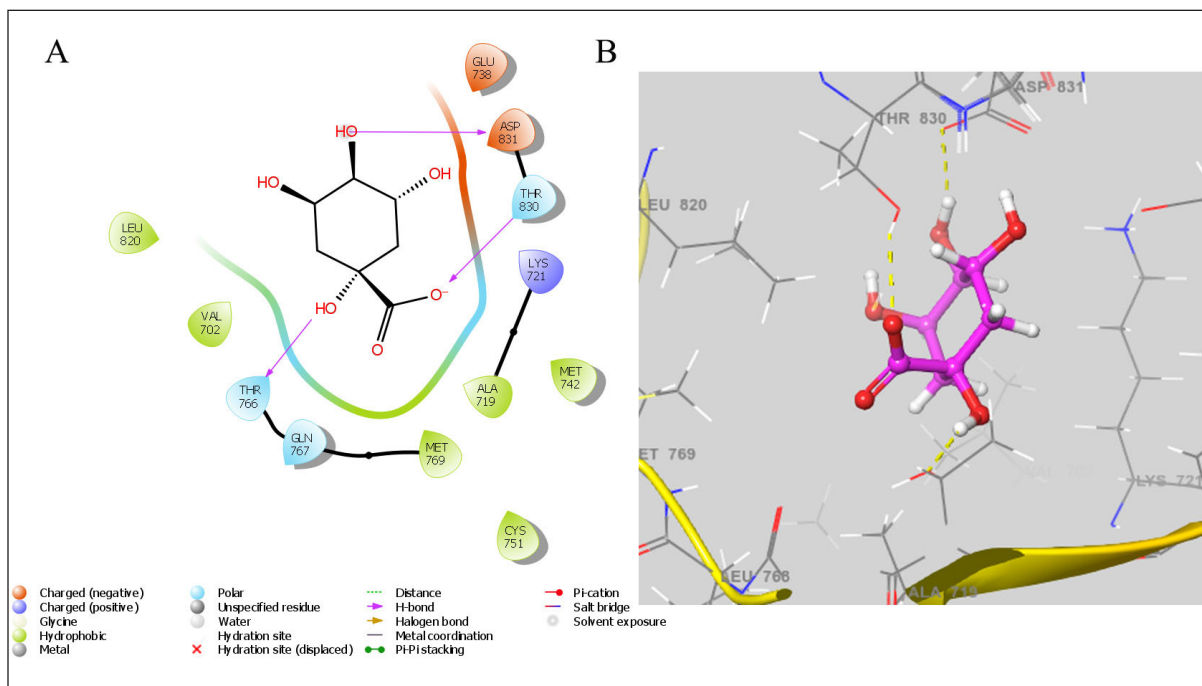


Figure 3. The estimated binding geometry of quinic acid on the active site of EGFR, (A and B) 2D and 3D structures of interaction.

proteins. It also showed a better docking score of -9.103 Kcal/mol, indicating better anticancer activity [30].

Anticancer activity

Various growth factors can engage with each other and be influenced by numerous phytoconstituents, which may also either activate or suppress cytokine signaling pathways. Like genistein, a phytoestrogen that inhibits the PI3K/AKT signaling

pathway in MCF-7 cells, may trigger apoptosis [18,31,32]. The AKT signaling pathway also suppresses the activity of NF- κ B in prostate cancer cells [33]. The EAML at varying concentrations demonstrated anticancer activity against the breast cancer cell lines MCF-7 and T47D in the MTT assay, yielding IC_{50} values of 76.64 ± 2.56 and 142.43 ± 1.86 μ g/ml, respectively, compared to the control (untreated cell lines). Figure 4 illustrates the dose-dependent cytotoxicity observed against the colorectal cancer

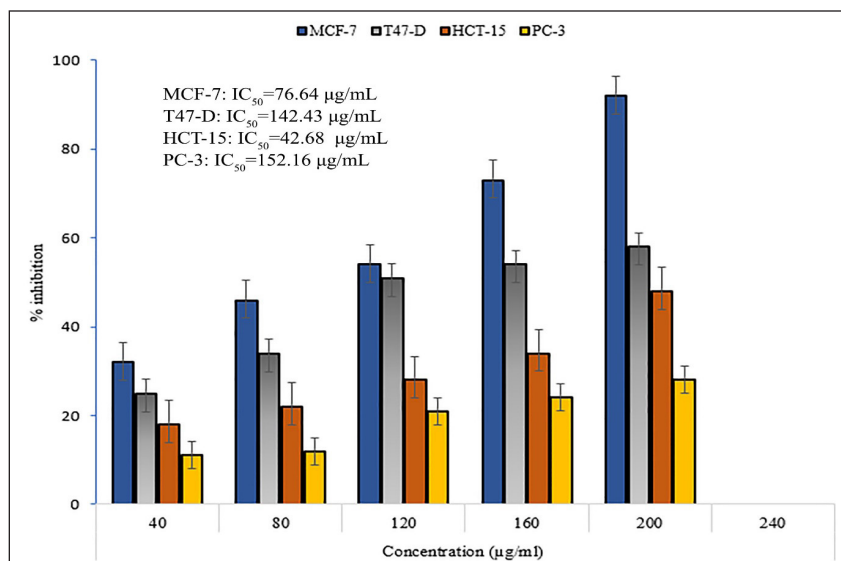


Figure 4. *Annona muricata* leaf extract shown anticancer efficacy on MCF-7, T47-D, HCT-15, and PC-3 cell lines using the MTT test. The values are expressed as mean \pm standard error ($n = 3$).

cell line HCT-15 and the prostate cancer cell line PC3, with IC_{50} values recorded at 42.68 ± 2.89 and 152.16 ± 3.21 $\mu\text{g/ml}$, respectively, compared to the control (untreated cell lines).

Figure 5 illustrates significant morphological changes in the experimental group, including shrinkage, detachment, membrane blebbing, and twisted form, which are absent in the control group. The control displayed a standard undamaged cellular architecture, and visual representations were captured using a Biorad Fluorescent microscope. In the process of apoptotic labeling, living cells display green fluorescence and retain a characteristic nuclear structure. Cells in the initial stages of programmed cell death exhibit fragmented nuclei and show yellow fluorescence alongside condensed chromatin. In the later phases of apoptosis, cells display an orange fluorescence attributed to condensed or fragmented chromatin, leading to cell nuclei that are consistently stained red/orange.

In silico ADME prediction

Lipinski's rule of five asserts that a chemical molecule demonstrating pharmacological or biological activity possesses five chemical and physical properties that enhance its effectiveness as an oral therapeutic agent in humans. The rule elucidates molecular attributes, including ADME, which are essential for a drug's pharmacokinetics inside the human body. Due to its high throughput and low cost, ADME modeling has drawn the attention of pharmaceutical researchers for the drug development process [34]. Various physicochemical properties were calculated, including the octanol/water partition coefficient, water/gas partition coefficient, brain/blood partition coefficient, donor hydrogen bond count, acceptor hydrogen bond count, and percentage of human oral absorption. These physicochemical properties are given in Table 2. The quinic acid ADME findings showed significant results in close accordance with the QikProp rule and Lipinski's rule of five.

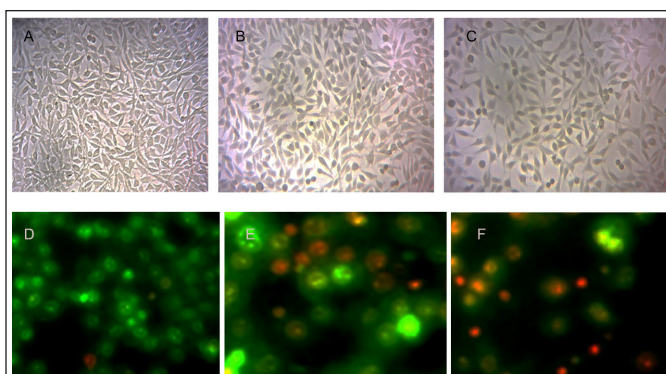


Figure 5. The photomicrograph displays the morphological changes in MCF-7 cells resulting from EAML treatment (Control $\mu\text{g/ml}$ (A), 200 $\mu\text{g/ml}$ (B), and 300 $\mu\text{g/ml}$ (C) for 24 hours). The images illustrate that the extract treatment leads to shrinkage, separation, membrane blebbing, and altered morphology when compared to the control group. The letters D, E, and F denote MCF-7 cancer cells subjected to extract at concentrations of 200 and 300 $\mu\text{g/ml}$ over a period of 24 hours. The cells were subsequently stained with a combination of dyes AO/EB and analyzed through fluorescence microscopy. Cells in the early stages of programmed cell death exhibit nuclei with fractures and yellow fluorescence due to constricted chromatin, while those in the later phases display orange fluorescence because of condensed or shattered chromatin.

Tomlinson *et al.* [34] were the first to describe FGFR3 mutations in bladder cancer. The extracellular domain of FGFR receptors comprises a hydrophobic signal peptide at the amino-terminal position, followed by three Ig-like domains, a hydrophobic transmembrane domain, and an intracellular tyrosine kinase domain. FGFs attach to extracellular Ig-like domains II and III, serving as ligands for FGFRs, which triggers downstream signaling [35].

The data revealed that quinic acid may downregulate the core protein levels and exhibit possible binding activity with associated target proteins. Numerous studies have shown EGFR mutations as a significant predictive biomarker

Table 2. Physicochemical properties of quinic acid.

Compound	QPlogP0/w ¹ *	QPlogPw *	QPlogKp *	QPlogBB ⁵ *	DonorHB *	AcceptHB *	Percent Human Oral Absorptio*
Quinic acid	-0.56	21.231	-4.867	-3.135	7	11.95	89.835

*The phytochemical properties include octanol/water partition coefficient, water/gas partition coefficient, brain/blood partition coefficient, donor hydrogen bond count, acceptor hydrogen bond count, and percentage of human oral absorption.

for EGFR tyrosine kinase responsiveness [36]. Patients with adenocarcinoma tumors, female gender, little cigarette smoking exposure, and Asian ethnicity have enhanced responses to EGFR TK inhibitors because of the increased prevalence of activating EGFR mutations in this cancer group [22,37]. Further studies are needed to confirm the mechanism of action.

CONCLUSION

The study explored the interaction between bioactive compounds from *A. muricata* leaves and EGFR proteins, revealing the presence of poly ketones as key components. In this investigation, a total of six bioactive metabolites were speculatively discovered, and from this, quinic acid showed inhibitory action on FGFR3 and EGFR proteins by forming hydrogen bonds. Most of these interactions occurred via hydrophobic amino acid residues. In the *in vitro* evaluation of anticancer activity, the extract showed a markable effect with IC₅₀ values, MCF-7-76.64 ± 2.56, T47D-142.43 ± 1.86, HCT-15-42.68 ± 2.89, and PC3-152.16 ± 3.21 µg/ml, respectively. The study's findings were corroborated by observed morphological alterations, including membrane blebbing, cell separation, and a rounder cell shape in comparison to parental cells. This research elucidates the anticancer profile screening of *A. muricata* leaves. To investigate the mechanism of action or the potential for clinical trials, more research is required.

LIST OF ABBREVIATIONS

ADMET, absorption, distribution, metabolism, excretion, and toxicity; AO, acridine orange; EAML, ethanolic extract of the *A. muricata* leaves; EB, ethidium bromide; EGFRs, epidermal growth factor receptors; ESI, electrospray ionization; FGFRs, fibroblast-growth factor receptors; Ig, immunoglobulin; MTT, 3-(4, 5-dimethylthiazol-2-yl)-2, 5-diphenyltetrazolium bromide; PDB, protein data bank; RMSD, root mean square deviation.

AUTHOR CONTRIBUTIONS

All authors made substantial contributions to conception and design, acquisition of data, or analysis and interpretation of data; took part in drafting the article or revising it critically for important intellectual content; agreed to submit to the current journal; gave final approval of the version to be published; and agree to be accountable for all aspects of the work. All the authors are eligible to be an author as per the International Committee of Medical Journal Editors (ICMJE) requirements/guidelines.

FINANCIAL SUPPORT

There is no funding to report.

CONFLICTS OF INTEREST

The authors report no financial or any other conflicts of interest in this work.

ETHICAL APPROVALS

This study does not involve experiments on animals or human subjects.

DATA AVAILABILITY

The authors affirm that the data substantiating the conclusions of this investigation are accessible inside the paper.

PUBLISHER'S NOTE

This journal remains neutral with regard to jurisdictional claims in published institutional affiliation.

REFERENCES

- Grossman HB, Natale RB, Tangen CM, Speights VO, Vogelzang NJ, Trump DL, *et al.* Neoadjuvant chemotherapy plus cystectomy compared with cystectomy alone for locally advanced bladder cancer. *N Engl J Med.* 2003 Aug 28;349(9):859–66.
- Moreira AL, Eng J. Personalized therapy for lung cancer. *Chest.* 2014 Dec 1;146(6):1649–57.
- Lemmon MA, Schlessinger J. Cell signalling by receptor tyrosine kinases. *Cell.* 2010 Jun 25;141(7):1117–34. doi: <https://doi.org/10.1016/j.cell.2010.06.011>
- Helsten T, Elkin S, Arthur E, Tomson BN, Carter J, Kurzrock R. The FGFR landscape in cancer: analysis of 4,853 tumours by next-generation sequencing. *Clin Cancer Res.* 2016 Jan 1;22(1):259–67. doi: <https://doi.org/10.1158/1078-0432.CCR-14-3212>
- Preusser M, Berghoff AS, Berger W, Ilhan-Mutlu A, Dinhof C, Widhalm G, *et al.* High rate of FGFR1 amplifications in brain metastases of squamous and non-squamous lung cancer. *Lung Cancer.* 2014 Jan 1;83(1):83–9. doi: <https://doi.org/10.1016/j.lungcan.2013.10.004>
- Ross JS, Wang K, Al-Rohil RN, Nazeer T, Sheehan CE, Otto GA, *et al.* Advanced urothelial carcinoma: next-generation sequencing reveals diverse genomic alterations and targets of therapy. *Mod Pathol.* 2014 Feb;27(2):271–80.
- Kawamata F, Patch AM, Nones K, Bond C, McKeone D, Pearson SA, *et al.* Copy number profiles of paired primary and metastatic colorectal cancers. *Oncotarget.* 2018 Jan 1;9(3):3394. doi: <https://doi.org/10.18632/oncotarget.23277>
- Edwards J, Krishna NS, Witton CJ, Bartlett JM. Gene amplifications associated with the development of hormone-resistant prostate cancer. *Clin Cancer Res.* 2003 Nov 1;9(14):5271–81.
- Petroni G, Buqué A, Coussens LM, Galluzzi L. Targeting oncogene and non-oncogene addiction to inflame the tumour microenvironment. *Nat Rev Drug Discov.* 2022 Jun;21(6):440–62.
- Touat M, Ileana E, Postel-Vinay S, André F, Soria JC. Targeting FGFR signalling in cancer. *Clin Cancer Res.* 2015 Jun 15;21(12):2684–94. doi: <https://doi.org/10.1158/1078-0432.CCR-14-2329>
- Katoh M. Therapeutics targeting FGF signalling network in human diseases. *Trends Pharmacol Sci.* 2016 Dec 1;37(12):1081–96. doi: <https://doi.org/10.1016/j.tips.2016.10.003>

12. Babina IS, Turner NC. Advances and challenges in targeting FGFR signalling in cancer. *Nat Rev Cancer*. 2017 May;17(5):318–32.
13. Ezirim AU, Okochi VI, James AB, Adebeshi OA, Ogunnowo S, Odeghe OB. Induction of apoptosis in myelogenous leukemic k562 cells by ethanolic leaf extract of *Annona muricata* L. *Glob J Res Med Plants Indig Med*. 2013 Mar 1;2(3):142.
14. Moghadamtousi SZ, Kadir HA, Paydar M, Rouhollahi E, Karimian H. *Annona muricata* leaves induced apoptosis in A549 cells through mitochondrial-mediated pathway and involvement of NF- κ B. *BMC Complement Altern Med*. 2014 Dec;14(1):1–3.
15. Pieme CA, Kumar SG, Dongmo MS, Moukette BM, Boyoum FF, Ngogang JY, *et al.* Antiproliferative activity and induction of apoptosis by *Annona muricata* (*Annonaceae*) extract on human cancer cells. *BMC Complement Altern Med*. 2014 Dec;14(1):1.
16. Dai Y, Hogan S, Schmelz EM, Ju YH, Canning C, Zhou K. Selective growth inhibition of human breast cancer cells by graviola fruit extract *in vitro* and *in vivo* involving downregulation of EGFR expression. *Nutr Cancer*. 2011 Jul 1;63(5):795–801. doi: <https://doi.org/10.1080/01635581.2011.563027>
17. de Pedro N, Cautain B, Melguizo A, Vicente F, Genilloud O, Peláez F, *et al.* Mitochondrial complex I inhibitors, acetogenins, induce HepG2 cell death through the induction of the complete apoptotic mitochondrial pathway. *J Bioenerg Biomembr*. 2013 Feb;45:153–64.
18. Suhail P, Venkatachalam V, Balasubramanian T, Christopher PV. A review on the *in vitro* anticancer potentials of acetogenins from *Annona muricata* Linn. a potential inducer of Bax-Bak and Caspase-3 related pathways. *Ind J Pharm Edu Res*. 2024 Aug 10;58(3s):s693–703. doi: <http://dx.doi.org/10.5530/ijper.58.3s.73>
19. Gavamukulya Y, Abou-Elella F, Wamunyokoli F, AEI-Shemy H. Phytochemical screening, anti-oxidant activity and *in vitro* anticancer potential of ethanolic and water leaves extracts of *Annona muricata* (Graviola). *Asian Pac J Trop Med*. 2014 Sep 1;7:S355–63.
20. Salac ELO, Alvarez MR, Gaurana RS, Grijaldo SJB, Serrano LM, Juan F, *et al.* Biological assay-guided fractionation and mass spectrometry-based metabolite profiling of *Annona muricata* L. Cytotoxic compounds against lung cancer A549 cell line. *Plants (Basel)*. 2022;11(18):2380. doi: <https://doi.org/10.3390/plants11182380>
21. Gavamukulya Y, Maina EN, Meroka AM, Madivoli ES, El-Shemy HA, Magoma G, *et al.* Liquid chromatography single quadrupole mass spectrometry (LC/SQ MS) analysis reveals presence of novel antineoplastic metabolites in ethanolic extracts of fruits and leaves of *Annona muricata*. *Pharmacognosy J*. 2019;11(4):660–8.
22. Sekine A, Kato T, Hagiwara E, Shinohara T, Komagata T, Iwasawa T, *et al.* Metastatic brain tumours from non-small cell lung cancer with EGFR mutations: distinguishing influence of exon 19 deletion on radiographic features. *Lung Cancer*. 2012 Jul 1;77(1):64–9. doi: <https://doi.org/10.1016/j.lungcan.2011.12.017>
23. Cinkilic N, Cetintas SK, Zorlu T, Vatan O, Yilmaz D, Cavas T, *et al.* Radioprotection by two phenolic compounds: chlorogenic and quinic acid, on X-ray induced DNA damage in human blood lymphocytes *in vitro*. *Food Chem Toxicol*. 2013 Mar 1;53:359–63. doi: <https://doi.org/10.1016/j.fct.2012.12.008>
24. Zhang W, Zhu XL, Ding W, Shi XX. A novel stereoselective synthesis of (–)-quinic acid starting from the naturally abundant (–)-shikimic acid. *Tetrahedron: Asymmetry*. 2015 Dec 15;26(23):1375–81. doi: <https://doi.org/10.1016/j.tetasy.2015.10.008>
25. Jänne PA, Yang JC, Kim DW, Planchard D, Ohe Y, Ramalingam SS, *et al.* AZD9291 in EGFR inhibitor-resistant non-small-cell lung cancer. *N Engl J Med*. 2015 Apr 30;372(18):1689–99. doi: <https://doi.org/10.1056/NEJMoa1411817>
26. Fajrin FA, Nugroho AE, Susilowati R, Nurrochmad A. Molecular docking analysis of ginger active compound on transient receptor potential cation channel subfamily V member 1 (TRPV1). *Indones J Chem*. 2018;18(1):179–85.
27. Suhail P, Venkatachalam VV, Joseph S, Murali R, Renganathan AB. *In vitro* anticancer potential and molecular modelling study of flavanol glucoside from graviola (*Annona muricata*) fruit: a potential inhibitor of antiapoptotic proteins. *Lett Appl NanoBioSci*. 2024;13(4):167.
28. Katoh M. Fibroblast growth factor receptors as treatment targets in clinical oncology. *Nat Rev Clin Oncol*. 2019 Feb;16(2):105–22.
29. Larsen JE, Minna JD. Molecular biology of lung cancer: clinical implications. *Clin Chest Med*. 2011 Dec 1;32(4):703–40. doi: <https://doi.org/10.1016/j.ccm.2011.08.003>
30. Luo J, Solimini NL, Elledge SJ. Principles of cancer therapy: oncogene and non-oncogene addiction. *Cell*. 2009 Mar 6;136(5):823–37. doi: <https://doi.org/10.1016/j.cell.2009.02.024>
31. Kamiloglu S, Sari G, Ozdal T, Capanoglu E. Guidelines for cell viability assays. *Food Front*. 2020 Sep;1(3):332–49.
32. Anastasius N, Boston S, Lacey M, Storing N, Whitehead SA. Evidence that low-dose, long-term genistein treatment inhibits oestradiol-stimulated growth in MCF-7 cells by down-regulation of the PI3-kinase/Akt signalling pathway. *J Steroid Biochem Mol Biol*. 2009;116(1–2):50–5. doi: <https://doi.org/10.1016/j.jsbmb.2009.04.009>
33. Li Y, Sarkar FH. Inhibition of nuclear factor kappa B activation in PC3 cells by genistein is mediated via Akt signaling pathway. *Clin Cancer Res*. 2002;8(7):2369–77.
34. Tomlinson DC, Baldo O, Harnden P, Knowles MA. FGFR3 protein expression and its relationship to mutation status and prognostic variables in bladder cancer. *J Pathol*. 2007 Sep;213(1):91–8.
35. Al-Obaidy KI, Cheng L. Fibroblast growth factor receptor (FGFR) gene: pathogenesis and treatment implications in urothelial carcinoma of the bladder. *J Clin Pathol*. 2021 Aug 1;74(8):491–5.
36. Aguilar-Serra J, Gimeno-Ballester V, Pastor-Clerigues A, Milara J, Trigo-Vicente C, Cortijo J. Cost-effectiveness analysis of the first-line EGFR-TKIs in patients with advanced EGFR-mutated non-small-cell lung cancer. *Expert Rev Pharmacoecon Outcomes Res*. 2022 May 19;22(4):637–46.
37. Wang P, Li Y, Lv D, Yang L, Ding L, Zhou J, *et al.* Mefatinib as first-line treatment of patients with advanced EGFR-mutant non-small-cell lung cancer: a phase Ib/II efficacy and biomarker study. *Signal Transduct Target Ther*. 2021 Nov 1;6(1):374.

How to cite this article:

Suhail P, Venkatachalam VV, Balasubramanian T, Murali R, Renganathan ABL. Evaluation of anticancer activity of *Annona muricata* leaf targeting FGFR3 and EGFR receptors against bladder and lung cancer. *J Appl Pharm Sci*. 2025;15(04):095–101.